

CURE: Privacy-Preserving Split Learning Done Right

Halil Ibrahim Kanpak*, Aqsa Shabbir†, Esra Genç†, Alptekin Küpçü*‡, Sinem Sav††

*Koç University, Istanbul, Turkey

†Bilkent University, Ankara, Turkey

‡Correspondence: akupcu@ku.edu.tr and sinem.sav@cs.bilkent.edu.tr

Abstract—Training deep neural networks often requires large-scale datasets, necessitating storage and processing on cloud servers due to computational constraints. The procedures must follow strict privacy regulations in domains like healthcare. Split Learning (SL), a framework that divides model layers between client(s) and server(s), is widely adopted for distributed model training. While Split Learning reduces privacy risks by limiting server access to the full parameter set, previous research has identified that intermediate outputs exchanged between server and client can compromise client’s data privacy. Homomorphic encryption (HE)-based solutions exist for this scenario but often impose prohibitive computational burdens.

To address these challenges, we propose CURE, a novel system based on HE, that encrypts *only* the server side of the model and optionally the data. CURE enables secure SL while substantially improving communication and parallelization through advanced packing techniques. We propose two packing schemes that consume one HE level for one-layer networks and generalize our solutions to n -layer neural networks. We demonstrate that CURE can achieve similar accuracy to plaintext SL while being $16\times$ more efficient in terms of the runtime compared to the state-of-the-art privacy-preserving alternatives.

I. INTRODUCTION

Big data has been a critical driving force behind the advancement of machine learning (ML). While enabling the training of more complex models in terms of prediction capability, massive dataset sizes create storage and processing bottlenecks that prohibit local computation on standard computers. More importantly, collecting, storing, and processing big data raises privacy concerns since the data often contains sensitive information. In addition to these inherent challenges, the data is often distributed among multiple parties, necessitating the use of collaborative ML methods.

Collaborative ML enables multiple parties to train a machine learning model without sharing raw data or, depending on the setting, the model itself. The most popular collaborative ML techniques include federated learning [33], [32], [45] and split learning [24]. Federated Learning (FL) enables multiple parties to train a machine learning model without sharing their local data directly. Instead, they share local model updates with a central server, which aggregates these updates to train a global model. Split Learning (SL), on the other hand, splits the neural network (NN) architecture into client-side and server-side models. Thus, it facilitates the training of NNs without sharing the data and/or labels with the server, especially in asymmetrical computational resource settings where clients may lack significant computational power.

Although FL and SL reduce privacy risks by restricting the server’s access to raw data or segments of the model, recent

research demonstrates that the client’s intermediate model updates, i.e., the gradients shared with the server, can still inadvertently leak sensitive information about the training data or the labels [54], [47], [21], [87], [43], [22], [26], [53], [18]. Researchers focused on developing new defense strategies to mitigate this leakage in FL using differential privacy (DP) [70], [36], [3], [46], [82], [83], homomorphic encryption (HE) [20], [69], [68], or secure multiparty computation (MPC) [27], [76], [92], [57], [58], [90], [64], [78], [79], [13], [93].

To mitigate various adversarial attacks in SL, several works rely on DP [73], [75], [5], [81], [85]. However, DP-based learning requires high privacy budgets, resulting in lower accuracy [63]. Another line of research employs HE for encrypted training or inference in the SL framework [56], [30], [31], [29]. While Pereteanu et al. integrate HE for *inference* tasks in SL [56], most efforts to improve privacy focus only on U-shaped split learning, where the neural network is divided into three segments: the client handles the initial and final layers, while the server processes the intermediate layers [30], [31], [29]. This setting assumes that the client holds its own data and labels, necessitating sufficient storage and computational capacity on the client side. To the best of our knowledge, there is no prior work that focuses on privacy-preserving training in the traditional split learning setting where the network is divided into two parts.

In this work, we address privacy-preserving training within a split learning framework where the server has direct access to the samples, while the client holds the labels. We protect the confidentiality of the labels and optionally the samples. This setting is motivated by scenarios where the client seeks to outsource the storage of samples and portions of the training computation. One plausible example of such a setting is large-scale genomic datasets. Genomic data, while often kept unencrypted, does not always reveal sensitive labels for complex traits like Autism Spectrum Disorder (ASD), influenced by numerous genomic variants affecting susceptibility genes [16], [67], [52]. The disorder’s heterogeneity and diverse genomic variants complicate its straightforward characterization and identification. Thus, even when stored in an unencrypted form on the server, the data itself does not disclose sensitive labels, but labels themselves constitute the important piece of information.

To achieve data and/or label confidentiality in the described setting, we propose a novel system, CURE, leveraging homomorphic encryption (HE) to encrypt the model parameters on the *server side only*. Thus, the server operates with an encrypted model while the client, the original owner of the data and/or labels, operates on a plaintext model. By

encrypting the server-side model, CURE mitigates privacy attacks from the server and ensures label privacy by default. Additionally, CURE optionally encrypts data samples, thereby further enhancing data privacy. This setup not only protects data and/or label privacy but also optimizes communication and computational overhead through plaintext training on the client side, making it particularly valuable in fields such as healthcare or genomics where data confidentiality is paramount.

Our contributions can be summarized as follows: (i) We introduce a novel system, CURE, for privacy-preserving split learning that ensures the confidentiality of labels and (optionally) the data using homomorphic encryption. (ii) We propose two packing schemes that ensure efficient computation under different settings, for one-level server operations. (iii) We generalize our packing to support encrypted multi-layer server models. (iv) We build an estimator that decides on where to best split the neural network to facilitate efficient use of CURE, tailored to the resources available on the server and client. (v) We evaluate our approach through extensive experiments and analysis, demonstrating superior performance compared to state-of-the-art methods with training times improved by up to $16\times$.

II. RELATED WORK

A. Split Learning

Split Learning (SL) [24] is a machine learning method that enables model training on distributed data sets without requiring the exchange of raw data among participants. It achieves this by splitting the machine learning model architecture into sections, each managed by a different party. SL first gained recognition with a distributed deep learning model called SplitNN [77] to help simplify the health entities to collaboratively train deep learning models without sharing raw sensitive data which is considered more resource-efficient than state-of-the-art collaborative machine learning methods such as federated learning [70], [33], [74]. This technique has opened up possibilities for various configurations designed to different practical health settings [37], [66], [60], [59], [28] offering configurations including the vanilla configuration [77], [42], [91] where the network is split into two parts from a specific cut layer. Each client trains a partial deep network independently, allowing for more secure and privacy-preserving machine learning applications. Additionally, vertical split learning [8], [6] involves different parties holding different features of the dataset [50], [51]. In contrast, horizontal split learning involves different dataset samples held by various parties to be processed independently [12], [62] to enhance query performance which refers to how quickly and effectively the system can distribute data across multiple parties by localizing data access.

Soon after SL gained recognition in the machine learning field, several attacks were developed to attain the raw data that is being processed through the split learning pipeline unveiling the critical privacy leakage issue to a spectrum of adversarial attacks, including inference attacks [54], [18], hijacking attacks [21], backdoor attacks [87], [89], feature distribution attacks [22], data reconstruction attacks [88], and property inference attack [53]. Thus, SL requires integration of further privacy mechanisms to mitigate the aforementioned attacks.

B. Privacy-Preserving Split Learning

To enhance privacy and eliminate various adversarial attacks, several works integrate a mechanism called differential privacy (DP) to SL [73], [75], [5], [81], [85]. DP adds noise to the data or intermediate values shared between client and server, thereby reducing the accuracy of the results. Our work distinguishes itself from DP-based approaches by integrating HE – a form of encryption that allows mathematical operations to be performed on encrypted data without the need to decrypt it – with split learning to eliminate the privacy vs. accuracy tradeoff.

Other works [56], [31], [30], [29] integrate the HE mechanism into the deep learning pipeline within SL. By encrypting data and/or model parameters with HE, any information obtained by attackers would be unusable without the decryption key, thus strengthening security and privacy in case of a compromise. For example, Pereteanu et al. [56] propose a solution leveraging Homomorphic Encryption and U-shaped split Convolutional Neural Networks (CNN) to ensure data privacy, specifically designed for fast and secure inference in computer vision applications. Their model enhances secure *inference* by distributing the model weights between the client and server with the client computation done in plaintext and the server computation done in encrypted form. In contrast, our approach focuses on the efficient and secure *training* of the model with advanced packing techniques to optimize communication and computational efficiency, allowing for collaborative model training while maintaining data and/or label confidentiality by encrypting server-side model parameters using an inverted traditional SL setup, with the server processes the initial layers of the neural network, and sends intermediate results to the client. The client then processes the subsequent layers in plaintext, completing the forward and backward propagation.

Khan et al. address the privacy challenge in SL by integrating HE directly into training to encrypt activation maps before sending them from the client to the server [31], [30], [29]. In their study, the authors developed a U-shaped split 1D CNN model, where the initial and the final layers reside on the client and the server processes the intermediate layers, to optimize the flow of information where the model begins with a public segment during training, then diverges into two branches, resembling the letter "U", to process public and private data separately [31]. These branches reconverge for the inference phase, completing the "U" shape. This design ensures that clients can maintain the privacy of their ground truth labels without sharing them with the server. In [30], the authors enhanced the model by ensuring that clients do not need to share their input training samples or ground truth labels with the server. Similarly, in [29], building on the previous works [31], [30], they extended their experiments in the proposed setting. They also introduced batch encryption to optimize memory usage and computational performance when handling encrypted data. These approaches minimize privacy leakage by encrypting activation maps in a different setting where the client holds both the data and labels. In contrast, our framework optimizes the training process by *applying HE exclusively to the server-side model parameters* within an inverted traditional SL setup, where the initial layers are processed by the server in

encryption and the subsequent layers by the client in plaintext. Our method effectively reduces the privacy risks associated with the intermediate outputs and gradients exchanged between the client and the server, achieving more efficient training compared to traditional techniques. This ensures minimal storage and computation on the client side, balancing privacy and efficiency.

In summary, while various approaches integrate HE into split learning to enhance privacy, our method uniquely focuses on optimizing training efficiency through HE applied solely to server-side model parameters. This approach effectively mitigates privacy risks associated with intermediate outputs and gradients, offering an efficient training solution.

III. BUILDING BLOCKS

In this section, we introduce the building blocks on which CURE relies on. We describe the neural networks, split learning, and the homomorphic encryption scheme we leverage.

A. Neural Networks

In the context of machine learning, a neural network (NN) is a computational model composed of interconnected nodes arranged in layers [4], [84], [17], [44]. During training, the network adjusts the weights of connections between neurons to minimize the loss, i.e. the difference between its predictions and labels (outcomes), using an optimization algorithm such as gradient descent. The input data (X) is passed through the network to produce a predicted output (\hat{Y}). Each neuron in the network performs a weighted sum of its inputs, applies an activation function, and passes the result to the neurons in the next layer. This process is called forward pass [15]. The forward pass thus requires activation on a linear combination of layer's weights with the activation values of the previous layer to predict the output (\hat{Y}) as $\hat{Y} = \psi(Z_l) = \psi(W_l O_{l-1} + B_l)$. Here, l is the current layer and O_{l-1} denotes the output of the previous layer $l-1$, ψ is the activation function, e.g., Sigmoid, Softmax, ReLU, W_l and B_l denote the weight matrix and the bias vector at layer l , respectively. We denote the linear combination of the weights and the activations as Z_l to facilitate the discussion on backpropagation below.

After the forward pass, backpropagation [65], [15] is performed to update the weights of the connections in the network by calculating a loss function (J) using the predicted output (\hat{Y}) and the labels (Y). Common loss functions include Mean Squared Error (MSE), Cross-Entropy Loss for classification, etc. The gradient of the loss function concerning the parameters of each layer is calculated by $g = \frac{\partial J}{\partial Z_l} = \frac{\partial J}{\partial \hat{Y}} \cdot \frac{\partial \hat{Y}}{\partial Z_l}$ where g is the gradient of the loss function with respect to the input Z_l at layer l . After computing the gradients [34], the parameters (weights and biases) are updated using the below formula to minimize the loss function: $W_l \leftarrow W_l - \alpha \frac{\partial J}{\partial W_l}$ and $B_l \leftarrow B_l - \alpha \frac{\partial J}{\partial B_l}$ where α is the learning rate.

B. Split Learning

Split Learning (SL) [77], [59], [91], [8], [24] is a technique designed to enhance data privacy while enabling collaborative model training across multiple entities. SL divides the NN

model between clients and a server, ensuring that raw data never leaves the client's side.

In SL, the NN model is divided into two segments: the client-side segment with k layers and the server-side segment with n layers. Each client processes its local data (X) through the first k layers of the model. The output from the k -th layer, denoted as O_k , is then transmitted to the server. Instead of transmitting raw data, this intermediate representation is used for subsequent computations. The server then continues the forward pass through the remaining n layers to compute the predicted output, denoted as \hat{Y} , which is used to evaluate the loss function (J). The server then computes the gradient of the loss with respect to \hat{Y} and sends it back to the clients. Each client uses this gradient to perform the backward pass through its k layers and update its model parameters accordingly. This iterative process of forward and backward passes, along with parameter updates, continues until the model converges or reaches a predefined number of epochs. For detailed explanation of our split learning architecture and its implementation, please see Section IV-C.

SL offers several advantages. Firstly, it enhances privacy since raw data remains on the client side, and only intermediate representations are shared. These representations are typically more abstract and less informative than the raw data, reducing the risk of sensitive information exposure. Secondly, SL reduces the computational load on the client side, as clients only handle the processing of k layers, which is computationally less expensive than training the entire model. This makes SL particularly suitable for devices with limited computational resources.

In conclusion, SL shows promise for achieving secure and efficient collaborative learning across diverse domains. However, adversarial attacks [54], [18], [21], [87], [89], [22], [39], [43], [26], [53], [47], [88] on SL continue to pose a threat. To address this, we aim to enhance the security and privacy of split learning by integrating HE, which we detail below.

C. Homomorphic Encryption

Homomorphic encryption (HE) is a cryptographic technique that allows computation on ciphertexts, generating encrypted results that, when decrypted, match the outcome of operations performed on the plaintext. This capability is crucial for privacy-preserving computations, allowing encrypted data to be processed without decryption, thus maintaining confidentiality. There are several HE schemes available, each with their strengths and weaknesses. For example, the Brakerski-Gentry-Vaikuntanathan (BGV) [11] and Brakerski/Fan-Vercauteren (BFV) [19] schemes are designed for performing arithmetic operations over integers or polynomials and offer strong security guarantees, but they can be less efficient for operations on real numbers with floating-point precision. For efficient floating-point arithmetic, we rely on the Cheon-Kim-Kim-Song (CKKS) scheme that is introduced below.

1) *Cheon-Kim-Kim-Song (CKKS) Scheme*: The CKKS scheme developed by Cheon et al. [14] is a leveled HE scheme based on the ring learning with errors (RLWE) problem [41]. The scheme is well-suited for supporting approximate (floating-point) precision. CKKS significantly enhances computational efficiency with its *packing capability*, enabling simultaneous

processing of multiple data points through Single Instruction, Multiple Data (SIMD) operations on encrypted data (see Section IV-E1 for details). The scheme also has effective noise management strategies, where the noise refers to the small error added to ciphertexts to ensure security, making it practical for tasks such as machine learning and data analysis. The ring in CKKS is defined as $\mathbb{Z}[X]/(X^N+1)$, where N is a power of two. Key parameters include the cyclotomic ring size (N), the ciphertext modulus (Q), the logarithm of the moduli of the ring ($\text{Log}QP$), the noise parameter (σ), and the level of the ciphertext (L) that help to manage the depth of the circuit to be evaluated before refreshing the ciphertext through $\text{Bootstrap}(c')$ that is detailed below. The scheme allows for packing $N/2$ values to plaintext/ciphertext slots for SIMD operations. The slots of the vector can be rearranged through an operation known as “rotations”, which can be computationally expensive. We introduce the key functionalities of the CKKS scheme here:

- $\text{KeyGen}(1^\lambda)$: Generates a pair of keys, a public key (PK) for encryption and a secret key (SK) for decryption, given a security parameter (λ).
- $\text{Enc}_{\text{PK}}(m)$: Encrypts a plaintext message (m) into ciphertext (c) using PK.
- $\text{Dec}_{\text{SK}}(c)$: Decrypts a ciphertext message (c) back into the plaintext message (m) using SK.
- $\text{Eval}_{\text{PK}}(c_a, c_b)$: Performs arithmetic operations such as addition and multiplication directly on ciphertexts (c_a, c_b), producing a new ciphertext that represents the result of the operation on the original plaintexts. Each multiplication consumes one level of the ciphertext.
- $\text{Bootstrap}(c)$: Refreshes ciphertexts (c) to produce a fresh ciphertext (c') at the initial level when all levels are consumed, allowing further operations without noise interference.

We denote encrypted ciphertext vectors in bold case, e.g., \mathbf{X} , and encoded plaintext vectors in regular case, e.g., X , throughout the paper.

IV. METHOD

A. Problem Statement

We consider a split learning setting where the model training is split between a server and a client. In this setup, the server has access to the data samples, denoted as X , but does not possess the labels, denoted as Y , which are known only to the client. This setting is motivated by a client who wishes to outsource storage and part of the computation to the server side. Our objective is to enable training within this split learning framework while maintaining the confidentiality of the labels and, optionally, the data samples. We note here that the reconstruction/inference attacks *on the client side* are out of the scope of this work as we assume the client is the owner of both samples and labels but outsources the storage of the samples and part of the processing.

B. Threat Model

We consider a semi-honest model without collusion between the server and the client. This is a plausible assumption

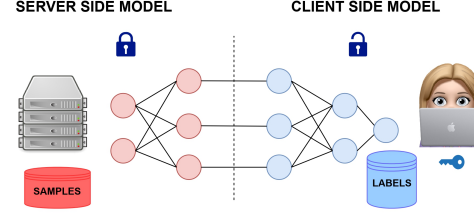


Figure 1: CURE System's Model. The server side (left) processes data samples \mathbf{X} with n layers, while the client side (right) holds the labels \mathbf{Y} and processes k layers of a neural network. Server-side weights \mathbf{W}_s are encrypted, while client-side weights W_c are unencrypted.

regarding our motivation that the client is the initial owner of the data samples, yet outsources the storage and parts of the computing. Our threat model suggests that the server might passively try to infer sensitive information, i.e. samples and/or labels, from the exchanged messages and the model parameters, but will adhere to the protocol rules and not actively inject malicious inputs. We aim to eliminate various types of input extraction attacks or membership inference attacks [71], [94], [54], [47]. These attacks typically exploit the intermediate computations and gradients shared during the training process to reconstruct sensitive data. By encrypting the server-side computations using HE, we ensure that the server cannot access any meaningful information from the encrypted data, thereby mitigating these attack vectors.

Algorithm 1 Initialization

```

1: function INITIALIZATION
2:   if client then
3:      $l_c \leftarrow [l_{n+1}, \dots, l_{n+k}]$  ▷ Client-side layers
4:      $W_c \leftarrow \text{GenRandomWeights}(l_c)$ 
5:      $(\text{PK}_c, \text{SK}_c) \leftarrow \text{KeyGen}(1^\lambda)$ 
6:     Send  $\text{PK}_c$  to server
7:   else if server then
8:      $l_s \leftarrow [l_1, l_2, \dots, l_n]$  ▷ Server-side layers
9:      $W_s \leftarrow \text{GenRandomWeights}(l_s)$ 
10:     $\mathbf{W}_s \leftarrow \text{Enc}_{\text{PK}_c}(W_s)$ 
11:   end if
12: end function

```

C. Overview of CURE:

We propose a novel framework, CURE, designed to facilitate split learning under the aforementioned threat model. Thus, CURE enables collaborative machine learning across client and server with asymmetric computational resources. We employ HE, in particular the CKKS scheme (see Section III-C), to allow computations to be performed on encrypted data, ensuring that sensitive information remains secret and eliminating attacks via communicated values throughout the training process. We illustrate the overview of CURE in Figure 1. Throughout the paper, we denote server-side and client-side parameters with a subscript of 's' and 'c', respectively.

The server is responsible for storing the data samples (\mathbf{X}) and performing forward pass computations ($f(\cdot)$) up to

Algorithm 2 CURE Training Phase

```
1: for epoch = 1  $\rightarrow$   $e$  do
2:   for  $\mathbf{X}_{[1,2,\dots,s]} \in \mathbf{X}$  do
3:     Server performs:
4:      $\mathbf{O}_n \leftarrow f(\mathbf{W}_s, \mathbf{X})$ 
5:     Send  $\mathbf{O}_n$  to client
6:     Client performs:
7:      $\mathbf{O}_n \leftarrow \text{Dec}_{\text{SK}_c}(\mathbf{O}_n)$ 
8:      $\hat{Y} \leftarrow f(W_c, \mathbf{O}_n)$ 
9:      $J \leftarrow \text{Loss}(\hat{Y}, Y)$ 
10:    Compute gradients  $g_{W_s}, g_{W_c}$ 
11:     $W_c \leftarrow \text{Update}(W_c, g_{W_c})$ 
12:     $\mathbf{g}_{W_s} \leftarrow \text{Enc}_{\text{PK}_c}(g_{W_s})$ 
13:    Send  $\mathbf{g}_{W_s}$  to server
14:    Server updates model:
15:     $\mathbf{W}_s \leftarrow \text{Update}(\mathbf{W}_s, \mathbf{g}_{W_s})$ 
16:  end for
17: end for
```

certain (n) layers. With server-side model parameters \mathbf{W}_s , the encrypted output (\mathbf{O}_n) is sent to the client, who then decrypts it and completes the forward pass ($f(\cdot)$) of the remaining (k) layers along with its parameters, denoted as W_c . The client, which holds the labels (Y), computes the loss (J) and its gradients (\mathbf{g}_{W_s}) and (g_{W_c}), updating W_c locally and sending the encrypted gradient (\mathbf{g}_{W_s}) back to the server. The server updates its parameters in an encrypted fashion provided by the client. This process ensures that (optionally) the data X and definitely the labels Y remain confidential, adhering to the objectives of our split learning framework.

Our protocols' security relies on the premise that the server, despite observing encrypted gradients communicated during the training, cannot deduce the underlying labels better than random guessing, provided that the HE scheme used effectively makes the encrypted values indistinguishable from random.

CURE's protocols are designed to ensure that all interactions and computations are conducted securely, leveraging HE to maintain data and/or label privacy throughout the machine learning process. This approach not only protects sensitive information but also allows for scalable and efficient distributed/outsourced learning, accommodating scenarios where participants have different levels of computational power and data sensitivity.

D. CURE's Design:

1) *Initialization*: This phase of CURE's framework, as detailed in Algorithm 1, is crucial for setting up the necessary cryptographic keys and model parameters for secure and efficient training. The initialization begins by defining the split model architecture, where l_s represents the server-side layers $[l_1, l_2, \dots, l_n]$ and l_c represents the client-side layers $[l_{n+1}, \dots, l_{n+k}]$. The client and the server randomly initialize their weights through $\text{GenRandomWeights}(l.)$ function that randomly initializes the weight matrices for a set of layers ($l.$) (Lines 4 and 9). The client also generates a pair of public and secret keys (PK_c, SK_c) using KeyGen operation of HE

scheme (Line 5), and then sends the public key (PK_c) to the server (Line 6). The server encrypts its weights (\mathbf{W}_s) using PK_c (Line 10). Thus, initialization ensures that the server-side weights are encrypted before any data exchange, maintaining privacy from the outset.

2) *Training*: The CURE training algorithm, as detailed in Algorithm 2, follows a systematic approach for privacy-preserving training using a split learning framework. First, the server performs the forward pass of n layers under encryption, either on encrypted data (\mathbf{X}) ensuring that the server never accesses raw (unencrypted) data, or on plaintext data X , depending on the application. We note that in the latter case, CURE only enables label confidentiality. At this step, the server computes a forward pass ($f(\cdot)$) on its model portion using the encrypted weights (\mathbf{W}_s) and the sample batch (\mathbf{X}) (Line 4), producing an encrypted output (\mathbf{O}_n) of n layers, which is then sent to the client (Line 5). Then, the client receives \mathbf{O}_n , decrypts it using its secret key (SK_c) (Line 7), and performs a forward pass ($f(\cdot)$) on its model portion using the decrypted output (\mathbf{O}_n) and its weights (W_c) (Line 8), resulting in the predicted output (\hat{Y}). The loss (J) is computed using \hat{Y} and the true labels (Y) (Line 9). The gradients for both client-side (g_{W_c}) and server-side (g_{W_s}) are calculated (Line 10). The client updates its weights (W_c) using its gradient (g_{W_c}) (Line 11), encrypts the server gradient (\mathbf{g}_{W_s}) with PK_c (Line 12), and sends it to the server (Line 13). Finally, upon receiving \mathbf{g}_{W_s} the server updates its \mathbf{W}_s accordingly (Line 15). This process repeats for each batch and continues for the predefined number of epochs (e), ensuring efficient and secure training of the model through collaborative computation between the client and server.

E. Method: Homomorphic Operations

In this section, we summarize how CURE relies on HE properties of CKKS and introduce our cryptographic optimizations to efficiently enable privacy-preserving split learning. In the realm of HE, optimizing computational efficiency is crucial due to the inherently high complexity of operations. In our work, with various cases, we have used various optimization approaches, considering resources and restrictions related to security and practicality. These approaches include packing, enhancing one-level operations ($n=1$), and avoiding resource-exhaustive operations whenever possible. In this section, we first summarize the packing capability of the CKKS scheme, then our one-level operations, and generalize our solutions to encrypted execution of n server layers. Lastly, we briefly explain our approximated activation functions and the bootstrapping operation to refresh ciphertexts.

1) *Packing*: Packing is the most general and applicable optimization used in our work. It involves using an RLWE interface vector as efficiently as possible. Due to its fundamental nature and simplicity, packing is widely employed in our approach. For a ring size of N , CKKS allows for packing $N/2$ values to plaintext/ciphertext slots (see Section III-C). This enables simultaneous operations on $N/2$ values through SIMD operations. For this, we identify similarities among the operations performed on data and encode (pack) similarly processed data within the same vector.

The following explanation outlines how we apply this principle through a toy example. Here d_{ij} represents the entries of an arbitrary matrix, β is a scalar multiplicative, and underscores represent garbage values. Consider D a 3×3 data matrix:

$$D = \begin{bmatrix} d_{00} & d_{01} & d_{02} \\ d_{10} & d_{11} & d_{12} \\ d_{20} & d_{21} & d_{22} \end{bmatrix}$$

Instead of performing a scalar multiplication in HE separately for each entry of the matrix as:

$$\begin{aligned} &\beta \cdot \begin{bmatrix} d_{00} & - & - & - & - & \dots & - \end{bmatrix} \\ &\beta \cdot \begin{bmatrix} d_{01} & - & - & - & - & \dots & - \end{bmatrix} \\ &\vdots \\ &\beta \cdot \begin{bmatrix} d_{22} & - & - & - & - & \dots & - \end{bmatrix} \end{aligned}$$

We pack and augment the data properly with respect to the operation to utilize the computational resources more efficiently. The packing is done as follows:

$$\beta \cdot [d_{00} \quad d_{01} \quad \dots \quad d_{22} \quad - \quad \dots \quad -]$$

By restructuring the data in this manner, we fill the RLWE vector with meaningful data and pad it with zeros when necessary, as discussed in Section IV-E3. This approach reduces the memory footprint and computational load by minimizing the number of operations and ciphertexts required. Consequently, choosing the right packing scheme enhances both the time and memory efficiency of HE operations.

2) *One-Level Operations*: In this section, we explain CURE's one-level operations, i.e., operations that consume only one level before decryption on the client side (before Line 7, Algorithm 2). Therefore, the number of server-side layers is one ($n=1$). These operations offer several advantages by consuming one level of a ciphertext. Overall, one-level operations produce less noise, leading to better accuracy both empirically and theoretically. This is because data is processed homomorphically only once, preventing noise accumulation. Consequently, processing data only once eliminates the need for bootstrapping, thereby reducing overall time.

In CURE, we utilize one-level operations when the network is split from the second layer, i.e., the server executes only the first layer with the encrypted weights. This particular splitting offers various advantages: (i) It minimizes data transfer and ensures that only the errors calculated by the client and the results of the products obtained by the server need to be transferred, (ii) it maintains one-level operations throughout CURE training, eliminating the need for bootstrapping operations. Therefore, we strongly recommend splitting from the first layer. However, CURE is a versatile solution, and we elaborate on our generic approach to n encrypted server layers in the next subsection. We detail our one-level plaintext-ciphertext multiplications below. Note that ciphertext-ciphertext operations are also one-level, but we explain our one-level operations on plaintext-ciphertext multiplication for simplicity.

Batch multiplication primarily involves element-wise multiplication of RLWE vectors, denoted as \odot , between plaintext and ciphertext elements. In contrast, scalar multiplication, denoted as \otimes , computes the product of each plaintext element with each

component of the ciphertext vector individually with scalar multiplication, obtaining the result by summing the vectors obtained from these scalar products. Let a and b be the arbitrary vectors with a being an encrypted ciphertext and b being a plaintext. Pairwise element batch multiplication can be represented as:

$$[a_0, a_1 \dots] \odot [b_0, b_1 \dots] = [a_0 b_0, a_1 b_1 \dots]$$

Scalar multiplication can be represented as:

$$a \otimes [b_0, b_1 \dots] = [ab_0, ab_1 \dots]$$

Although scalar multiplication demonstrates faster computation—approximately 2.7 times faster in our experiments—batch multiplication offers superior utilization of packing, resulting in better throughput (indeed, for single layer operations, we do not even need a fully homomorphic encryption scheme, but packing provides superior efficiency overall). Therefore, we propose the one-level batch and one-level scalar methods, incorporating packing in both approaches. Firstly, in one-level batch multiplication, we pack weight matrices as batches of columns, enabling matrix-vector multiplication using ciphertext-plaintext operations exclusively. This matrix initialization on the second layer is crucial for optimization. By forming the weight matrix to be packed, the dimensions of the first two layers will determine the packing efficiency with respect to the number of slots an RLWE vector has. It is important to note that this packing is non-trivial and is highly dependent on the dataset, parameters of the HE scheme, and restrictions imposed by security concerns and computational resources. To use batch multiplication, one must properly pack the encrypted weight matrix and multiply it with plaintext as indicated in our method, which can be costly in the cases that we discuss in Section V-C. However, batch multiplication allows us to utilize packing more effectively, resulting in improved performance. The number of slots and the column length of the weight matrix compensate for the additional time caused by the inherent latency of batch multiplication. In cases where the weight matrix behaves better with packing, the transformed weight matrix compensates for the additional time required for batch multiplication compared to scalar multiplication by exclusively operating on columns with packing.

In contrast, for one-level scalar multiplication, there is no need for such preprocessing on the components of the network except for the encoding and encryption of the elements. However, since one-level scalar multiplication cannot utilize packing as efficiently as one-level batch multiplication, there is a possibility of higher demand for memory and computation in some cases. Therefore, it is important to carefully decide which one-level operation to use, considering the trade-offs.

It is important to note that, although we distinguish between scalar and batch in their names, we utilize packing in both operations. In both methods, each column of the weight matrices is stored using batch encoding. However, in the one-level scalar method, a single column is stored in a single ciphertext, whereas, in the one-level batch method, multiple columns are stored in the same ciphertext, allowing for better packing efficiency in the scenarios discussed earlier.

To calculate the multiplication of a 4×4 matrix with a 4-dimensional vector, the operations can be summarized as:

$$\begin{bmatrix} a_{11} & a_{12} & a_{13} & a_{14} \\ a_{21} & a_{22} & a_{23} & a_{24} \\ a_{31} & a_{32} & a_{33} & a_{34} \\ a_{41} & a_{42} & a_{43} & a_{44} \end{bmatrix} \times \begin{bmatrix} b_1 \\ b_2 \\ b_3 \\ b_4 \end{bmatrix} = \begin{bmatrix} a_{11}b_1 + a_{12}b_2 + a_{13}b_3 + a_{14}b_4 \\ a_{21}b_1 + a_{22}b_2 + a_{23}b_3 + a_{24}b_4 \\ a_{31}b_1 + a_{32}b_2 + a_{33}b_3 + a_{34}b_4 \\ a_{41}b_1 + a_{42}b_2 + a_{43}b_3 + a_{44}b_4 \end{bmatrix}$$

Our one-level batch multiplication is represented as:

$$= \begin{bmatrix} b_1 \\ b_1 \\ b_1 \\ b_1 \end{bmatrix} \odot \begin{bmatrix} a_{11} \\ a_{21} \\ a_{31} \\ a_{41} \end{bmatrix} + \begin{bmatrix} b_2 \\ b_2 \\ b_2 \\ b_2 \end{bmatrix} \odot \begin{bmatrix} a_{12} \\ a_{22} \\ a_{32} \\ a_{42} \end{bmatrix} + \begin{bmatrix} b_3 \\ b_3 \\ b_3 \\ b_3 \end{bmatrix} \odot \begin{bmatrix} a_{13} \\ a_{23} \\ a_{33} \\ a_{43} \end{bmatrix} + \begin{bmatrix} b_4 \\ b_4 \\ b_4 \\ b_4 \end{bmatrix} \odot \begin{bmatrix} a_{14} \\ a_{24} \\ a_{34} \\ a_{44} \end{bmatrix}$$

And our one-level scalar multiplication is represented as:

$$= b_1 \otimes \begin{bmatrix} a_{11} \\ a_{21} \\ a_{31} \\ a_{41} \end{bmatrix} + b_2 \otimes \begin{bmatrix} a_{12} \\ a_{22} \\ a_{32} \\ a_{42} \end{bmatrix} + b_3 \otimes \begin{bmatrix} a_{13} \\ a_{23} \\ a_{33} \\ a_{43} \end{bmatrix} + b_4 \otimes \begin{bmatrix} a_{14} \\ a_{24} \\ a_{34} \\ a_{44} \end{bmatrix}$$

Notice that the column-wise multiplication can be done in a batch or scalar fashion. In other words, we can write the multiplication of a column as scalar multiplication of b_i or element-wise vector multiplication with repeated elements of b_i as an RLWE-packed vector. When the ciphertext batch size is larger than the column size (e.g., two columns fit in one RLWE vector), we can utilize packing more efficiently for the one-level batch multiplication operation, as follows:

$$\begin{bmatrix} b_1 \\ b_1 \\ b_1 \\ b_1 \\ b_2 \\ b_2 \\ b_2 \\ b_2 \end{bmatrix} \odot \begin{bmatrix} a_{11} \\ a_{21} \\ a_{31} \\ a_{41} \\ a_{12} \\ a_{22} \\ a_{32} \\ a_{42} \end{bmatrix} + \begin{bmatrix} b_3 \\ b_3 \\ b_3 \\ b_3 \\ b_4 \\ b_4 \\ b_4 \\ b_4 \end{bmatrix} \odot \begin{bmatrix} a_{13} \\ a_{23} \\ a_{33} \\ a_{43} \\ a_{14} \\ a_{24} \\ a_{34} \\ a_{44} \end{bmatrix} = \begin{bmatrix} a_{11}b_1 + a_{13}b_3 \\ a_{21}b_1 + a_{23}b_3 \\ a_{31}b_1 + a_{33}b_3 \\ a_{41}b_1 + a_{43}b_3 \\ a_{12}b_2 + a_{14}b_4 \\ a_{22}b_2 + a_{24}b_4 \\ a_{32}b_2 + a_{34}b_4 \\ a_{42}b_2 + a_{44}b_4 \end{bmatrix}$$

Upon receiving the ciphertext, the client decrypts it and calculates:

$$\begin{bmatrix} a_{11}b_1 + a_{13}b_3 \\ a_{21}b_1 + a_{23}b_3 \\ a_{31}b_1 + a_{33}b_3 \\ a_{41}b_1 + a_{43}b_3 \end{bmatrix} + \begin{bmatrix} a_{12}b_2 + a_{14}b_4 \\ a_{22}b_2 + a_{24}b_4 \\ a_{32}b_2 + a_{34}b_4 \\ a_{42}b_2 + a_{44}b_4 \end{bmatrix} = \begin{bmatrix} a_{11}b_1 + a_{12}b_2 + a_{13}b_3 + a_{14}b_4 \\ a_{21}b_1 + a_{22}b_2 + a_{23}b_3 + a_{24}b_4 \\ a_{31}b_1 + a_{32}b_2 + a_{33}b_3 + a_{34}b_4 \\ a_{41}b_1 + a_{42}b_2 + a_{43}b_3 + a_{44}b_4 \end{bmatrix}$$

Our proposed methods differ from each other in the equations we have shown above and require modified implementations for different ratios of $\frac{N/2}{|l_2|}$ where $N/2$ is the number of slots and $|l_2|$ is the size of the second layer considering the weight matrix obtained by the first two layers. The determination of this ratio will also be important on the transaction layer of the network from the server to the client in case of n -layer encryption, as it is where we perform one-level operations. If the size of the second layer is large enough to leverage the improved packing utilization and the efficiency of scalar multiplication of RLWE vectors compared to batch multiplication, the one-level scalar approach is preferable. Conversely, when the size of the second layer is small, the one-level batch approach is more advantageous. More explicit decision thresholds are given in Section IV-F.

3) *Execution of n -encrypted layer networks and matrix-matrix operations:* In this subsection, we briefly explain CURE with multiple encrypted server layers. In an edge case, CURE allows for the execution of all layers of a network under encryption on the server side, except for the last layer (to hide the labels from the server), when the client has

extremely low computational power. It is important to note that in such a split learning setup, while the overall computational demand increases, it accommodates the client's computational limitations, ensuring training proceeds despite the client's capability. Overall, CURE empowers users to choose where to split, i.e., the number of encrypted layers, optimizing the balance between security, latency, and computational resources.

In settings with more than one encrypted layer, as opposed to one-level operations, several computational challenges arise due to the requirement for an HE product function for matrix-matrix multiplications. This includes performing ciphertext-ciphertext weight matrix multiplications on the server side, which leads to noise accumulation and the need for bootstrapping (see Section IV-E5), encrypted execution of activation functions (see Section IV-E4), increased computational demand, and potentially lower expected accuracy. Therefore, we introduce additional optimizations for implementing CURE in this complex setting in an efficient manner.

Firstly, we employ log-scaling operations to compute the inner products of vectors during matrix-matrix multiplications. This method involves summing vector elements by shifting them as powers of 2 and performing in-place rotations to simplify the multiplicative depth in HE operations. This approach effectively reduces computational overhead and noise induced by HE operations.

Additionally, for vector addition, multiplication, and scalar multiplication, we employ related packing strategies to further enhance efficiency for the inner product of vectors. Packing not only optimizes memory usage by consolidating data but also reduces the number of separate computational steps required, thereby accelerating the overall processing speed.

Our packing method for matrix-matrix multiplication involves two main steps. First, we determine how the columns of the second matrix will be placed on the RLWE interface for computation. We start by padding the columns of the second matrix with zeros to the nearest larger power of two. After padding, we concatenate the columns until they fill one RLWE interface vector. If a column is longer than the slot sizes, we repeat the padding and division process until each segment fits into one RLWE interface vector.

Once the columns are packed, we define the number of "division steps" as $\frac{N/2}{|B|}$ where $|B|$ is the size of the column matrix B . We mark the positions on the RLWE vectors in increments of this step size. For long columns that do not fit into a single RLWE vector, we calculate this quotient to ensure the correct summation of dot products for those column-row pairs. Here is a toy example of this process:

$$B = \begin{bmatrix} b_{00} & b_{01} & b_{02} & b_{03} & b_{04} \\ b_{10} & b_{11} & b_{12} & b_{13} & b_{14} \\ b_{20} & b_{21} & b_{22} & b_{23} & b_{24} \end{bmatrix}$$

First, we pad our matrix to achieve an efficient homomorphic dot product with optimized rotations.

$$\begin{bmatrix} b_{00} & b_{01} & & b_{04} \\ b_{10} & b_{11} & & b_{14} \\ b_{20} & b_{21} & \cdots & b_{24} \\ 0 & 0 & & 0 \end{bmatrix}$$

By concatenating and marking the entries, we achieve the placement of columns to the RLWE vectors for the dot product.

$$\begin{bmatrix} b_{00} \\ b_{10} \\ b_{20} \\ 0 \\ b_{01} \\ b_{11} \\ b_{21} \\ 0 \end{bmatrix} \begin{bmatrix} b_{02} \\ b_{12} \\ b_{22} \\ 0 \\ b_{03} \\ b_{13} \\ b_{23} \\ 0 \end{bmatrix} \begin{bmatrix} b_{04} \\ b_{14} \\ b_{24} \\ 0 \\ 0 \\ 0 \\ 0 \\ 0 \end{bmatrix}$$

After preparing the second vector, we process the rows of the first matrix by padding them to the nearest power of two and repeating the rows as necessary. We then calculate the homomorphic dot product for each column and extract the previously marked data. It is important to note that this marking operation serves as an abstraction for explanatory purposes.

$$\mathbf{A} = \begin{bmatrix} a_{00} & a_{11} & a_{02} \\ a_{10} & a_{11} & a_{12} \\ a_{20} & a_{21} & a_{22} \end{bmatrix}$$

To prepare the first row for the homomorphic dot product calculation, we arrange the elements as $[a_{00}, a_{10}, a_{20}, 0, a_{00}, a_{00}, a_{00}, 0, \dots]$ as a column vector. Next, we perform element-wise multiplication of this vector with the columns obtained from matrix \mathbf{B} . Subsequently, we rotate the resulting vector by powers of two until we cover all slots. After each rotation, we perform an element-wise addition with the previously accumulated vector. This process ultimately yields the dot product of the initial matrices' row-column pairs homomorphically, enabling efficient computation of the matrix-matrix product. Importantly, all operations from this stage onward are executed homomorphically.

$$\begin{bmatrix} b_{00} \\ b_{10} \\ b_{20} \\ 0 \\ b_{01} \\ b_{11} \\ b_{21} \\ 0 \end{bmatrix} \odot \begin{bmatrix} a_{00} \\ a_{10} \\ a_{20} \\ 0 \\ a_{01} \\ a_{10} \\ a_{21} \\ 0 \end{bmatrix} = \begin{bmatrix} a_{00} * b_{00} \\ a_{10} * b_{10} \\ a_{20} * b_{20} \\ 0 * 0 \\ a_{01} * b_{02} \\ a_{10} * b_{11} \\ a_{21} * b_{21} \\ 0 * 0 \end{bmatrix}$$

Next, we rotate and add the result to itself $\log n - 1$ times, ultimately achieving the desired outcome:

$$\begin{bmatrix} a_{00} * b_{00} \\ a_{10} * b_{10} \\ a_{20} * b_{20} \\ 0 * 0 \\ a_{01} * b_{02} \\ a_{10} * b_{11} \\ a_{21} * b_{21} \\ 0 * 0 \end{bmatrix} + \begin{bmatrix} a_{10} * b_{10} \\ a_{20} * b_{20} \\ 0 * 0 \\ a_{01} * b_{02} \\ a_{10} * b_{11} \\ a_{21} * b_{21} \\ 0 * 0 \\ a_{00} * b_{00} \end{bmatrix} = \begin{bmatrix} a_{00} * b_{00} + a_{10} * b_{10} \\ a_{10} * b_{10} + a_{20} * b_{20} \\ a_{20} * b_{20} + 0 * 0 \\ 0 * 0 + a_{01} * b_{02} \\ a_{01} * b_{02} + a_{10} * b_{11} \\ a_{10} * b_{11} + a_{21} * b_{21} \\ a_{21} * b_{21} + 0 * 0 \\ 0 * 0 + a_{00} * b_{00} \end{bmatrix}$$

Rotation of the this vector twice and addition will result in:

$$\begin{bmatrix} a_{00} * b_{00} + a_{10} * b_{10} \\ a_{10} * b_{10} + a_{20} * b_{20} \\ a_{20} * b_{20} + 0 * 0 \\ 0 * 0 + a_{01} * b_{02} \\ a_{01} * b_{02} + a_{10} * b_{11} \\ a_{10} * b_{11} + a_{21} * b_{21} \\ a_{21} * b_{21} + 0 * 0 \\ 0 * 0 + a_{00} * b_{00} \end{bmatrix} + \begin{bmatrix} a_{20} * b_{20} + 0 * 0 \\ 0 * 0 + a_{01} * b_{02} \\ a_{01} * b_{02} + a_{10} * b_{11} \\ a_{10} * b_{11} + a_{21} * b_{21} \\ a_{21} * b_{21} + 0 * 0 \\ 0 * 0 + a_{00} * b_{00} \\ a_{00} * b_{00} + a_{10} * b_{10} \\ a_{10} * b_{10} + a_{20} * b_{20} \end{bmatrix}$$

$$= \begin{bmatrix} a_{00} * b_{00} + a_{10} * b_{10} + a_{20} * b_{20} + 0 * 0 \\ a_{10} * b_{10} + a_{20} * b_{20} + 0 * 0 + a_{01} * b_{02} \\ a_{20} * b_{20} + 0 * 0 + a_{01} * b_{02} + a_{10} * b_{11} \\ 0 * 0 + a_{01} * b_{02} + a_{10} * b_{11} + a_{21} * b_{21} \\ a_{01} * b_{02} + a_{10} * b_{11} + a_{21} * b_{21} + 0 * 0 \\ a_{10} * b_{11} + a_{21} * b_{21} + 0 * 0 + a_{00} * b_{00} \\ a_{21} * b_{21} + 0 * 0 + a_{00} * b_{00} + a_{10} * b_{10} \\ 0 * 0 + a_{00} * b_{00} + a_{10} * b_{10} + a_{20} * b_{20} \end{bmatrix}$$

Note that the first and fifth entries of the final vector represent the desired homomorphic and efficient results of the first row's first column and the first row's second column of the resulting matrix. By proceeding with this process for each column and row, we can obtain the complete matrix-matrix product. For matrices with columns that do not fit into a single RLWE vector, we perform additional summation operations on the final result, based on the initial slot-to-column length ratio calculation.

With our optimized implementation of the homomorphic inner product of vectors, we can efficiently calculate the product of two matrices. This capability allows us to delegate more layers to the server, enhancing ciphertext-ciphertext operations up to the last layer, which was our goal. When the training phase of CURE reaches the server's last layer, we treat the network as a single-layer encrypted network and perform the appropriate one-level operation in that final layer.

4) *Approximated Activation Functions*: Due to the fully encrypted nature of the server layers, for n encrypted server layers where $n > 1$, the activation functions of $n - 1$ layers should also be executed under encryption. However, non-linear activation functions cannot be directly applied under encryption; only polynomial functions can be used. To address this limitation, we rely on well-known approximation techniques such as Chebyshev interpolation method [61] or minimax approximation [72] to approximate the non-linear activation functions as polynomials. This technique is also employed by numerous privacy-preserving machine learning works [69], [9], [23], [68], [20], [25], [38].

It is important to note that using higher-degree polynomials may result in better approximations and thus better accuracy. However, higher-degree polynomials also lead to more HE multiplications, resulting in noise accumulation and potentially necessitating bootstrapping as each multiplication consumes one ciphertext level. For a degree d polynomial, the scheme consumes $\log_2(d+1)$ levels. This results in increased computational complexity and can lead to higher training latency. Therefore, careful consideration is required when selecting the function and the degree of the polynomial used for the approximation.

5) *Bootstrapping*: For an initial level of L , CKKS allows for at most L multiplications to be carried out. As encrypted data undergoes multiple operations, noise accumulates, potentially making ciphertexts undecipherable. Thus, after L multiplications, **Bootstrap**(c) function (see Section III-C1) should be executed to refresh the ciphertext level to continue operating on that ciphertext. In CURE, we rely on bootstrapping operations when necessary. This occurs when the combined number of encrypted layers n and the degree of the activation function d consumes all available levels, i.e., when $(\log_2(d+1))n + n > L$. Note that in practice, it is possible to use different degrees of approximation for different server layers regarding activation functions (and even different activation functions). Bootstrap-

ping is necessary when their total degree, plus the number of server-side layers exceed the allowed number of multiplications.

F. Server-Client Estimator

In this section, we build an estimator to facilitate more effective utilization of CURE. This estimator function takes as input the key properties that impact the performance of CURE in a split learning network. These properties include the desired training time (T_d), computer specifications to calculate the latency of rotations to be computed, the depth of the multiplicative circuit (μ), the number of bootstrapping functions (γ), and the network bandwidth (\mathcal{O}_c) available between the client and the server, for a given network architecture and the machines used in training execution. We chose these properties because the number of rotations to be computed is one of the most time-consuming homomorphic operations, based on our microbenchmarks. This makes rotations the key operation affecting overall training latency. Similarly, just as rotations impact computation time, μ is the most significant parameter for accuracy. Along with properties related to time and accuracy, CURE also provides recommendations for training in scenarios where the client's computational power is low or where communication capabilities are limited.

Based on the computational capabilities of the given server and client devices, network bandwidth, and μ , the CURE estimator provides users with the recommended maximum values for the parameters they can choose for their NNs (number of server and client layers, size of server and client layers, degree of approximated polynomial activation functions). This is done by calculating the time rotations take with formula 1 according to a microbenchmark on one rotation operation, allowing them to reorganize their networks accordingly.

The estimator checks whether the desired training time can be achieved based on the total length and number of layers on the server side of the NN. It then provides recommendations accordingly. Let l_i be the i^{th} server layer and we will denote the size of that layer as $|l_i|$, we define $|\bar{l}_i|$ as the smallest power of two that is larger than $|l_i|$: $|\bar{l}_i| = \min\{2^k | 2^k > |l_i|\}$. For a network processing one sample in one pass, the number of rotations required for all encrypted matrix-matrix multiplication operations is given by:

$$\sum_{i=0}^n \left(\frac{|\bar{l}_i| \times |\bar{l}_{i+1}|}{N/2} \right) \times \log(|\bar{l}_{i+1}|) \quad (1)$$

Using this formula, a microbenchmark on the CKKS rotation operation estimator can estimate the time required for training to complete, considering the number of data points and the pre-defined number of epochs. Hence, the estimator suggests server-side specifications for the network based on user data regarding the maximum time one epoch will take. A typical NN estimator also calculates the network specifications for the given computational resources of the client, but without accounting for any homomorphic operations. Similarly, independent of the machines used in training, the estimator updates the network regarding the accuracy demands and depth of operations based on user data.

As an example, we can execute the estimator on **Model 1** from Section V-A5 that has 4 layers with $784 \times 128 \times 32 \times 10$ neurons. In our setup, we specified the machine configurations

in Section V-A2. The user inputs the required parameters as mentioned. For a longer desired maximum training time specified by the user, the estimator might suggest greater flexibility with the network configuration. For example, it could recommend increasing the size of the layers of **Model 1** for different applications or proposing additional server layers for the model, resulting in a configuration similar to **Model 2**. Similarly, for a shorter desired training time or a less complex operations configuration, the estimator may suggest 0 rotations with an additional base time for training, resulting in a one-level operations case with $n=2$, as defined in Section V-A5.

The estimator also considers the network specifications and suggests a maximum length for the server's last layer, which is a critical factor for the communication overhead. Based on our calculations in Section V-A2, users can adjust the server's last layer to optimize communication for their specific application. As an example, a ciphertext with a parameter set of $N=2^{13}$ is approximately 0.0078125 megabytes. We first calculate the amount of data to be transferred for a given network. The key parameters are the size of one RLWE interface vector and the number of these vectors needed to transfer data optimally for the given network. We propose the following formula:

$$\frac{|X| \times |l_n|}{N/2} \times |c| \quad (2)$$

where $|X|$ and $|l_n|$ denote the number of data samples and the size of the last server layer, respectively. $N/2$ is the number of slots and $|c|$ is the memory size of a ciphertext. Thus, for the **Model 1** network, the required data transfer, using this formula we obtain in V-A3, results in approximately 2.44140625 megabytes of data to be transferred per epoch. At a network rate of 1 MBps, the total communication time is also about 2.44140625 seconds. Based on this calculation, the estimator might suggest reducing the size of the server's last layer. This would decrease the dimensionality, allowing more layers for packing and, consequently, fewer ciphertexts to be transferred to the client.

V. EXPERIMENTAL EVALUATION

In this section, we experimentally evaluate CURE under various settings. First, we describe our experimental setup, followed by a detailed presentation of experimental results, including model accuracy and runtime performance with scalability analysis. Lastly, we provide a comparison with prior work.

A. Experimental Setup

1) *Implementation Details*: For our end-to-end experiments, we use the Go programming language [1], version 1.20.5. We chose Go for its compiler-based execution, which facilitates easy deployment on servers, and its support for parallel programming, essential for our encrypted experiments. Additionally, Go's compatibility with the robust and consistent Lattigo library made it our preferred choice for handling HE tasks. We employ Lattigo [2] version 5.0.2 cryptographic operations.

We also simulate CURE using the Python Pytorch [55] library, using approximated activation functions, CKKS noise [14] addition on encrypted layer calculations, and fixed-precision for encrypted layers to expedite accuracy experiments

(see Section V-B1). Using simulations allowed us to cross-validate our results obtained in Go and to forecast the accuracy of some of the networks and datasets in a timely manner. We note here that while we evaluate the correctness of our encrypted implementation, we rely on simulations to expedite accuracy tests in Section V-B1, as our main focus is optimizing the HE-based split learning pipeline. All our experiments were repeated twice and the average numbers are provided.

2) *Experimental Setup*: We experiment on an Ubuntu 18.04.6 LTS server with a 40-core Intel Xeon Processor E5-2650 v3 2.3GHz CPU 251GB of RAM for the evaluation of CURE. We used parallelization on our networks for both server-side and client-side calculations on this machine. Additionally, we experimented with varying the number of cores utilized during execution to obtain a broader range of results for analysis. We use two set of cryptographic parameters. **Set 1**: We use $N=2^{14}$ as CKKS ring size and $\log QP=438$, which represents the logarithm of the number of moduli in the ring. The scale is 2^{30} . This setting allows us to encrypt vectors of size $N/2 = 2^{13}$ into one ciphertext employing packing capability for the use of SIMD. **Set 2**: We use $N = 2^{13}$ and $\log QP = 218$. The scale is 2^{30} . This setting allows us to encrypt vectors of size $N/2 = 2^{12}$. We chose our default parameters to achieve 128-bit security according to the HE standard whitepaper [7].

3) *Network Setup*: We use MPI (Message Passing Interface) which is a standard for passing messages between different processes in a distributed memory system [48], enabling parallel computing architectures to communicate efficiently, to implement the communication between client and server. The experiments are conducted on LAN and WAN environments. We have two configurations for CURE server and client applications: one where both are located in local processes on a host server and another where they are on two different host machines in a WAN environment. Our primary focus was on LAN results because, for CURE, the determining factor is the computational expense of the HE operations. Finally, we extrapolate WAN results, by calculating the amount of data to be transferred for a given network through our estimator in Section IV-F (see formula 2, the left-hand side multiplicand represents the approximate number of data that need to be transferred depending on our packing methods discussed in Section IV-E).

4) *Datasets*: We employ various datasets for our accuracy evaluation: (i) Breast Cancer Wisconsin dataset (BCW) [10] with 699 samples, 9 features and 2 labels, (ii) the hand-written digits (MNIST) dataset [35] with 70,000 images of 28×28 pixels and 10 labels, (iii) the default of credit card clients (CREDIT) dataset [86] with $n=30,000$ samples, 23 features and 2 labels, (iv) the PTB XL dataset [80] (PTB-XL) with 21,837 clinical 12-lead ECG records, 10-second recordings with 100 Hz sampling rate, annotated with up to 71 different diagnostic classes. For the runtime and scalability evaluations, we use both the MNIST dataset and synthetic data with varying numbers of features and samples. This allows us to demonstrate how CURE behaves under different datasets and, more specifically, how one-level operations, ciphertext-ciphertext matrix products, and activation functions perform in different scenarios.

We employ the sigmoid activation function for unencrypted

| Network | Dataset | CURE Accuracy | Plaintext Accuracy |
|--------------------------|---------|---------------|--------------------|
| [input]x128x32x[output] | MNIST | 95.97% | 95.83% |
| | BCW | 97.37% | 98.25% |
| | CREDIT | 81.61% | 81.70% |
| [input]x1024x32x[output] | MNIST | 96.11% | 96.16% |
| | BCW | 98.25% | 99.12% |
| | CREDIT | 81.73% | 81.77% |
| [input]x2048x32x[output] | MNIST | 95.74% | 96.32% |
| | BCW | 99.12% | 99.12% |
| | CREDIT | 81.16% | 81.25% |

TABLE I: CURE’s accuracy results for plaintext and encrypted learning with 10 epochs.

layers and achieve a polynomial sigmoid approximation through Chebyshev interpolation [61] or minimax approximation [72], enabling activation functions under encryption on the server side. When approximating the sigmoid activation, we experimented with several different degree and interval values and we have decided that a degree value of 7 and an interval of $[-15, 15]$ strikes a sufficient balance between accuracy and efficiency. These baselines enable us to evaluate CURE’s accuracy loss due to the approximation of the activation functions, fixed precision, encryption, and the impact of privacy-preserving split learning.

5) *Model Architectures and Split Learning Setup*: We employ varying network models for our different types of experiments. The models are structured as follows: For time latency experiments we have used models; **Model 1**: $784 \times 128 \times 32 \times 10$ (adapted from [40]), **Model 2**: $784 \times 128 \times 128 \times 128 \times 128 \times 128 \times 128 \times 32 \times 10$, **Model 3**: $8192 \times 8192 \times 1024 \times 512 \times 128 \times 32 \times 10$, and **Model 4**: $16384 \times 16384 \times 8192 \times 32 \times 10$ and for simulation tests to obtain accuracy results we have used models; **Model 5**: $[input] \times 128 \times 32 \times [output]$, **Model 6**: $[input] \times 1024 \times 32 \times [output]$, **Model 7**: $[input] \times 2048 \times 32 \times [output]$ where [input] and [output] are the number of input and outputs in the respective datasets. The structure of these networks is designed to clearly demonstrate how the proposed methods perform across various settings. Unless otherwise stated, we use a batch size (b) of 60 for a fair comparison with [40]. We also experiment with various batch sizes to empirically show the effect of b on the runtime. Using our first four models for time latency experiments, we created several split learning setups for a chosen NN architecture to demonstrate how CURE provides advantages in different scenarios. We achieved this by varying n , which refers to the number of encrypted layers or, in other words, the position of the last layer of the server in the entire NN. We observe that n is a crucial determinant in the performance as it represents the network layers where the server homomorphically executes operations, as discussed in Section IV-E.

B. Experimental Results

1) *Model Accuracy*: Table I displays the accuracy results on various datasets. For all baselines, we use NN structures of **Models 5, 6, and 7** and the same learning parameters as CURE. We use the sigmoid as the activation for all layers in the network. For the baseline, we use the original sigmoid function, while for the encrypted version, we use the approximated version of the sigmoid.

| Model | Server Layers | Client Layers | Data Amount | Batch Size (b) | Execution Time LAN (m) | Execution Time WAN (m) |
|----------------|---|---|-------------|--------------------|------------------------|------------------------|
| Model 1 | 784×128 | 32×10 | 10,000 | 60 | 29.216 | 29.256 |
| Model 1 | 784×128 | 32×10 | 10,000 | 128 | 23.821 | 23.861 |
| Model 2 | 784×128 | $128 \times 128 \times 128 \times 128 \times 128 \times 32 \times 10$ | 10,000 | 60 | 35.703 | 35.743 |
| Model 2 | $784 \times 128 \times 128$ | $128 \times 128 \times 128 \times 128 \times 32 \times 10$ | 10,000 | 60 | 42.995 | 43.035 |
| Model 2 | $784 \times 128 \times 128 \times 128$ | $128 \times 128 \times 128 \times 32 \times 10$ | 10,000 | 60 | 49.923 | 49.963 |
| Model 2 | $784 \times 128 \times 128 \times 128 \times 128$ | $128 \times 128 \times 32 \times 10$ | 10,000 | 60 | 53.727 | 53.767 |
| Model 2 | $784 \times 128 \times 128 \times 128 \times 128 \times 128$ | $128 \times 32 \times 10$ | 10,000 | 60 | 58.202 | 58.242 |
| Model 2 | $784 \times 128 \times 128 \times 128 \times 128 \times 128 \times 128$ | 32×10 | 10,000 | 60 | 62.608 | 62.648 |
| Model 3 | 8192×8192 | $1024 \times 512 \times 128 \times 32 \times 10$ | 100 | 60 | 331.774 | 334.378 |
| Model 3 | $8192 \times 8192 \times 1024$ | $512 \times 128 \times 32 \times 10$ | 100 | 60 | 342.733 | 343.058 |
| Model 3 | $8192 \times 8192 \times 1024 \times 512$ | $128 \times 32 \times 10$ | 100 | 60 | 351.760 | 351.928 |
| Model 3 | $8192 \times 8192 \times 1024 \times 512 \times 128$ | 32×10 | 100 | 60 | 362.473 | 362.520 |
| Model 4 | 16384×16384 | $8192 \times 32 \times 10$ | 100 | 60 | 1183.345 | 1188.553 |
| Model 4 | 16384×16384 | $8192 \times 32 \times 10$ | 100 | 128 | 925.156 | 930.364 |
| Model 4 | 16384×16384 | $8192 \times 32 \times 10$ | 100 | 256 | 784.802 | 790.010 |
| Model 4 | 16384×16384 | $8192 \times 32 \times 10$ | 100 | 1024 | 615.381 | 620.589 |

TABLE II: CURE’s runtime for one training epoch (forward and backward passes to cover all data) with various NN architectures. Server layers are encrypted and parallelization on a 40-core CPU machine is used. We use the cryptographic parameter **Set 2** with $N = 2^{13}$ and extrapolate WAN results based on the estimations derived in Section V-A3 for a network with 1 Mbps bandwidth.

We observe that the accuracy loss between plaintext and CURE is between 0.04% and 0.6% when encryption is simulated. For example, CURE achieves 97.37% training accuracy on the BCW dataset, which is only %0.08 lower than the plaintext learning in terms of accuracy loss. Moreover, it should be noted that these training results are obtained using the same number of epoch iterations for a fair comparison. Therefore, the accuracy loss could be further reduced if the model is trained with a higher number of epochs using CURE.

2) *Model Time Latency:* In this section, we experiment with various NN architectures and various distributions of server and client layers to observe their effect on the training runtime, as detailed in Table II. The table presents the runtime of one epoch of various combinations of server and client layers. The server layers are encrypted. We vary the number of neurons in each layer, e.g., server layers 784×128 indicate an input layer of size 784 followed by a layer of 128 neurons. We use 100 or 10,000 samples with batch sizes of 60, 128, 256, 1024 to cover an extensive range of networks.

Effect of the number of server layers (n). We observe in Table II that with the increasing number of server layers, the runtime increases. This is due to the computationally demanding nature of homomorphic operations, which are primarily executed on the server.

Note that some rows, e.g., rows 3-8, describe the same network with different n ranging from 2 to 7, illustrating how CURE behaves under different network splits and emphasizing that HE operations are the primary determinant of time latency. Here, we aim to demonstrate the effect of different sequences of HE operations discussed in Section IV-E. Considering the first 6 rows for **Model 2** and the subsequent 4 rows for **Model 3** one can observe the impact of n on training time latency. Variations in n demand different numbers of matrix-matrix products to

be executed, thereby influencing the overall training time.

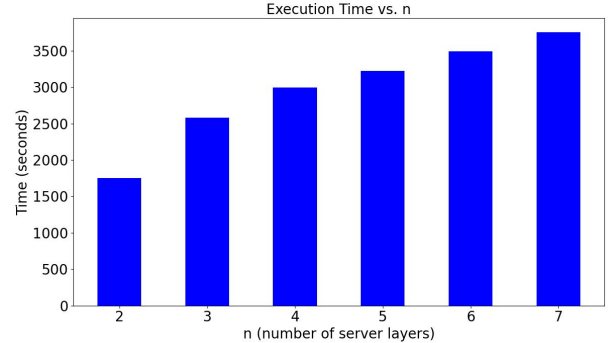


Figure 2: CURE’s runtime for one epoch on **Model 2**, with $b = 60$ and 40 CPU cores with varying n , excluding the bootstrapping time.

We observe that the addition of a third encrypted layer to the server significantly increases time latency for our experimental setting. This is due to the involvement of ciphertext-ciphertext operations, approximated activation functions, and subsequent bootstrapping required for the given cryptographic parameters (with $N = 2^{13}$). Adding further layers also increases the training time as expected while reducing the computational and memory load on the client. The additional time induced by adding a layer ranges from $1.0758\times$ to $1.204\times$ of the original, with the highest increase occurring on the third layer of the server, as mentioned. Note that when a different set of cryptographic parameters is used, this observation of the third layer may vary to some other layer. Similarly, for **Model 3**, we observe a similar pattern, with runtime increasing in the range of $1.0263\times$ to $1.330\times$, again with the highest increment occurring on the third layer addition to the server. Similar results can be observed in Figure 2

| Batch Size (b) | #CPU cores | Execution Time (m) |
|--------------------|------------|--------------------|
| 60 | 1 | 62.5 |
| 60 | 2 | 51.0 |
| 60 | 10 | 23.3 |
| 60 | 20 | 24.2 |
| 60 | 30 | 27.6 |
| 60 | 40 | 29.2 |
| 128 | 1 | 131.3 |
| 128 | 2 | 92.2 |
| 128 | 10 | 29.1 |
| 128 | 20 | 23.5 |
| 128 | 30 | 24.9 |
| 128 | 40 | 23.5 |

TABLE III: CURE’s runtime for one training epoch with 10,000 samples, **Model 1** network with the varying number of b and CPU cores. The first two layers are encrypted ($n=2$) on a LAN setting.

which displays the runtime of one epoch with **Model 1** when the network is split from the second layer leaving the third and fourth layers to the client, i.e., only the first layer is being encrypted. We use a $b=60$ with parallelization on the server side.

Effect of the batch size (b). The influence of b on training duration is also evident, where larger b generally reduce training times by optimizing the use of computational resources and reducing the overhead associated with managing many smaller batches. This finding highlights the CURE’s capability to handle larger batches more efficiently. We can observe in the first 2 rows (**Model 1**) and last 4 rows (**Model 4**) of Table II that increasing layer sizes improves the time latency of training when incrementing b . Doubling the b leads to a reduction in time latency ranging from $0.848\times$ to $0.718\times$. Although we use a $b=60$ for **Model 1** to ensure a fair comparison with [40] (see Section V-C), we found that varying b yield better results in terms of training time latency. b is also highly related to training time latency performance. With higher concurrency utilization, we have empirically observed that increasing b improves performance results in terms of training time latency. Conversely, the impact of performance degradation due to the increased number of CPU cores used diminishes and eventually vanishes as the b increases.

Effect of the neural network (NN) architecture. Moreover, Table II includes results from setups with different complexities of network structures - from simpler models with fewer layers to more complex ones with many layers. The results demonstrate a manageable increase in training times for more complex models, indicating that the CURE framework efficiently handles increased computational demands. We can see that even with large network sizes, CURE achieves practically applicable training times in most cases.

Effect of the number of cores. The scalability of the model is further tested through variations in the number of CPU cores utilized during training. Table III illustrates the impact of the number of CPU cores used on the runtime. It is observed that a greater number of cores drastically decreases training times, effectively leveraging parallel computation capabilities. We

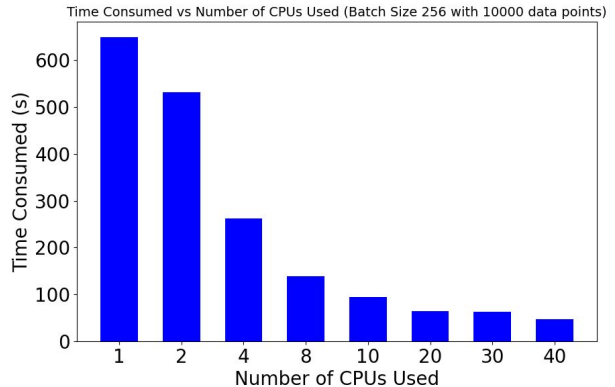


Figure 3: CURE’s runtime on **Model 1** for one epoch with 10,000 samples and $b=256$ with varying numbers of CPUs on a LAN setting.

observe in Table III that increasing the number of cores used in training provides a time latency advantage ranging from $2.204\times$ to $0.215\times$. It is important to note that, particularly in small networks (i.e., networks with a small number of layers that exhibit different behaviors for HE operations in a parallelized setup), increasing the number of cores does not necessarily improve the runtime performance. In some cases, it may even decrease the performance due to race conditions.

We observe that CURE is affected by the number of cores used in execution and batch size (b) simultaneously. Table III displays that $b=60$ and $b=128$ exhibit different trends for the varying number of CPUs used in the execution. This is important for deciding b in training, considering computational constraints and the nature of the training. It is noteworthy that larger b yields better results with an increasing number of CPUs, whereas smaller b performs better with fewer CPUs. This behavior in time latency with an increasing number of CPUs used for training a network is not present with larger b . Figure 3 shows the training of **Model 1** with $n=2$, $k=2$, using 10,000 samples and a batch size b of 256. We observe that while the improvement in performance is not as pronounced when changing the number of CPUs from 2 to 4 compared to changes from 20 to 30 or 30 to 40, there is no penalty in performance. This indicates that the number of CPUs when using larger b in training is not an important determinant. Furthermore, it suggests that users may achieve better results by increasing b while expanding the number of cores used in execution.

Table II also indicates that configurations where the server handles a heavier computational load benefit from the parallelization achieved. By leveraging the server’s superior processing power to efficiently manage encrypted data operations, we balance the computational burden more favorably compared to client-side processing. These insights, combined with the analysis summarized in Section IV-F, underscore the significance of architectural decisions in optimizing training processes and highlight CURE’s robust handling of computational complexities in a privacy-focused learning environment.

Effect of the number of samples. CURE also scales well with respect to the number of samples used in training.

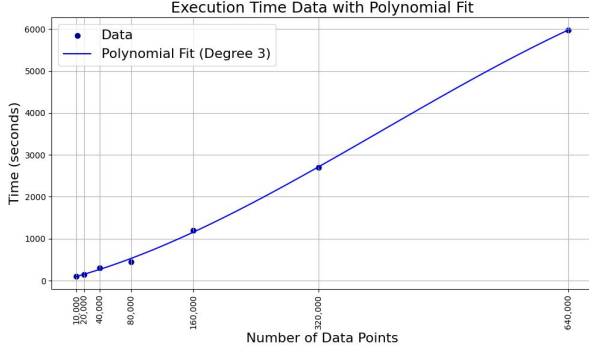


Figure 4: Homomorphic dot product scalability with respect to increasing number of data samples.

We have measured this scalability by considering only the homomorphic ciphertext-ciphertext dot product mentioned in Section IV-E. Figure 4 displays the effect of increasing number of samples when matrices of dimensions 1×2^{13} and $2^{13} \times$ number of samples taken into dot product we have implemented. By doubling the number of samples to be processed and recording the timing results, we have empirically observed a linear growth in the complexity of our ciphertext-ciphertext dot product.

C. Comparison with Prior Work

Comparing CURE with existing privacy-preserving split learning solutions is challenging due to its unique approach. To the best of our knowledge, there is no prior work that studies the inverted traditional SL setting of CURE. Our qualitative analysis primarily focuses on the efficiencies and overhead introduced by different frameworks (see Section II for details). CURE reduces communication costs by only transferring encrypted intermediate gradients, significantly optimizing the process by concentrating encrypted computations on the server side. This approach leverages the server’s robust computational capabilities, allowing for more efficient encrypted data handling and reducing the computational burden on clients. By minimizing homomorphic operations and communication overhead, CURE achieves superior time efficiency and accuracy.

As there is no prior work within the same split learning setting, we choose HE-based training methods that focus on fully encrypted training for comparison. CURE employs a unique training paradigm that restricts encrypted training to predefined server-side layers in the network. Thus, CURE also supports fully encrypted training when the number of server-side encrypted layers n equals the number of layers in the network, leading to a fair comparison. We choose two works of fully encrypted training [40], [49] and one privacy-preserving split learning framework [31] for the comparison and provide the results in Table IV. The values are derived from the papers as reported, and thus are not necessarily on the same machine configurations. Papers [40], [49], [31] conducted their experiments on machines with the following specifications: an Intel Xeon E7-8890 v4 2.2GHz CPU with 256GB DRAM, featuring two sockets with 12 cores each and supporting 24 threads; an Intel Xeon E5-2698 v3 Haswell processor with

| System | Data Set | Time Latency (h) |
|------------------------|----------|------------------|
| CURE (LAN) | MNIST | 8.3205 |
| CURE (LAN) One-level | MNIST | 4.8693 |
| Glyph (LAN)[40] | MNIST | 134.2592 |
| Nandakumar (LAN) [49] | MNIST | 111.1100 |
| CURE (LAN) | PTB XL | 34.5825 |
| CURE (WAN) | PTB XL | 34.5826 |
| Khan et al. (LAN) [31] | PTB XL | 20.1483 |
| Khan et al. (WAN) [31] | PTB XL | 341.3683 |

TABLE IV: The comparison with [40], [49], [31] with a fully encrypted network for 1 epoch with 10,000 MNIST samples and 10 epochs with 21,837 samples PTB-XL dataset. For the comparison against [31], we employ our one-level operations. We extrapolate our 1 epoch results to 10 epochs on the PTB-XL dataset, assuming a network bandwidth of 100 MBps. Note that we were unable to replicate the experiments from other papers on the same machine, so the training time latencies, with and without communication, are approximate values derived from those papers.

two sockets and sixteen cores per socket, running at 2.30GHz, equipped with 250GB of main memory; and a machine with an Intel Core i7-8700 CPU at 3.20GHz, 32GB RAM, and a GeForce GTX 1070 Ti GPU with 8GB of memory.

In Glyph [40], a fully encrypted setting requires 134 hours per epoch, while in CURE, the same setting (fully encrypted) takes approximately 8 hours per epoch, making CURE $16\times$ faster in the worst-case scenario. Notably, in the best case, CURE can achieve $64\times$ faster execution for the same task compared to [40] due to enabling the same task by encrypting only parts of the network on the server side with the same privacy guarantees. CURE also has the advantage on a WAN setting compared to [31] achieving $10\times$ faster execution.

VI. DISCUSSION

Based on our experimental evaluation, the scalar multiplication method performs consistently well in one-level operations, regardless of the size of the second layer. In contrast, the one-level batch method’s performance deteriorates with increasing second layer size. A practical heuristic for estimating packing method performance is given by $\frac{N/2}{|l_2|}$ where $N/2$ is the number of slots and $|l_2|$ is the size of the second layer. If this ratio is less than ~ 2.7 , the scalar multiplication method is preferable. It is also important to note that the size of the first layer affects both methods linearly since the matrices are stored column-wise.

Our comparison with the prior work [40] shows that CURE is faster than the state of the art. The proposed one-level batch method is $16\times$ and the one-level scalar method is $2.4\times$ faster than Glyph [40]. Additionally, we have shown that by adjusting batch size during training and the number of CPUs used in execution, users may achieve even better results. CURE also achieves accuracy levels on par with baseline (plaintext) or fully-encrypted approaches.

CURE excels in various tasks due to its innovative approach to privacy-preserving split learning. It effectively mitigates reconstruction attacks through encrypted gradients. Our novel

one-level operations reduce noise, enhancing the overall accuracy. Moreover, CURE incorporates bootstrapping for various network configurations with higher circuit depths, and our empirical results demonstrate successful implementation and superior performance. CURE also transfers a minimal amount of data per epoch. This efficiency is achieved by only exchanging the server's last layer and the client's first layer gradients per iteration. Consequently, CURE minimizes data transfer by leveraging the NN architecture's tendency to reduce data dimensionality. Additionally, CURE scales well with an increasing number of samples used in training. Quantitative descriptions of these results are discussed in Section V-B2.

We have also demonstrated that CURE is more broadly applicable to generic, n -layer networks. These innovations enable users to allocate more encrypted layers to the server, thereby reducing computational and memory loads on the client side and expanding the feasibility of real-world applications. The applicability of CURE's operations extends beyond resource allocation to different training scenarios. CURE achieves practical results with complex networks.

VII. CONCLUSION

We presented CURE, a novel and efficient privacy-preserving split learning framework that offers substantial improvements over previous methods. CURE is the first framework that encrypts only the server-side parameters, enabling secure outsourcing of storage and computational tasks from the client while ensuring the confidentiality of labels and optionally data samples. This approach effectively mitigates reconstruction attacks. By relying on our proposed packing strategies, CURE further enhances performance and outperforms fully encrypted training methods while achieving accuracy levels on par with both baseline and fully encrypted approaches. In conclusion, CURE not only enhances data security through encrypted server-side computations but also demonstrates practicality and broad applicability across diverse training scenarios and complex network architectures.

REFERENCES

- [1] Go Programming Language. <https://golang.org>. (Accessed: 2024-05-05).
- [2] Lattigo v5. Online: <https://github.com/tuneinsight/lattigo>, Nov. 2023. EPFL-LDS, Tune Insight SA.
- [3] M. Abadi, A. Chu, I. Goodfellow, H. B. McMahan, I. Mironov, K. Talwar, and L. Zhang. Deep learning with differential privacy. In *ACM CCS*, 2016.
- [4] O. I. Abiodun, A. Jantan, A. E. Omolara, K. V. Dada, N. A. Mohamed, and H. Arshad. State-of-the-art in artificial neural network applications: A survey. *Heliyon*, 4(11), 2018.
- [5] S. Abuadba, K. Kim, M. Kim, C. Thapa, S. A. Camtepe, Y. Gao, H. Kim, and S. Nepal. Can we use split learning on 1d cnn models for privacy preserving training? In *Proceedings of the 15th ACM Asia conference on computer and communications security*, pages 305–318, 2020.
- [6] O. S. Ads, M. M. Alfares, and M. A.-M. Salem. Multi-limb Split Learning for Tumor Classification on Vertically Distributed Data. In *ICICIS*, pages 88–92. IEEE, 2021.
- [7] M. Albrecht et al. Homomorphic Encryption Security Standard. Technical report, HomomorphicEncryption.org, 2018.
- [8] C. G. Allaart, B. Keyser, H. Bal, and A. Van Halteren. Vertical Split Learning - an exploration of predictive performance in medical and other use cases. In *IJCNN*, pages 1–8. IEEE, 2022.
- [9] M. Bakshi and M. Last. Cryptornn - privacy-preserving recurrent neural networks using homomorphic encryption. In *CSCML*, pages 245–253, 2020.
- [10] Breast cancer wisconsin (original). [https://archive.ics.uci.edu/ml/datasets/breast+cancer+wisconsin+\(original\)](https://archive.ics.uci.edu/ml/datasets/breast+cancer+wisconsin+(original)). (Accessed: 2024-05-05).
- [11] Z. Brakerski, C. Gentry, and V. Vaikuntanathan. (leveled) fully homomorphic encryption without bootstrapping. *ACM Transactions on Computation Theory (TOCT)*, 6(3):1–36, 2014.
- [12] S. Ceri, M. Negri, and G. Pelagatti. Horizontal data partitioning in database design. In *Proceedings of the 1982 ACM SIGMOD international conference on Management of data*, pages 128–136, 1982.
- [13] T. Chen and S. Zhong. Privacy-preserving backpropagation neural network learning. *IEEE Transactions on Neural Networks*, 20(10):1554–1564, Oct 2009.
- [14] J. H. Cheon, A. Kim, M. Kim, and Y. Song. Homomorphic Encryption for Arithmetic of Approximate Numbers. In *Advances in Cryptology – ASIACRYPT 2017*, pages 409–437. Springer International Publishing, 2017.
- [15] M. Cilimkovic. Neural Networks and Back Propagation Algorithm. *Institute of Technology Blanchardstown*, 15(1), 2015.
- [16] S. De Rubeis, X. He, A. P. Goldberg, C. S. Poultney, K. Samocha, A. Ercument Cicek, Y. Kou, L. Liu, M. Fromer, S. Walker, et al. Synaptic, transcriptional and chromatin genes disrupted in autism. *Nature*, 515(7526):209–215, 2014.
- [17] A. Dongare, R. Kharde, A. D. Kachare, et al. Introduction to Artificial Neural Network. *IJEIT*, 2(1):189–194, 2012.
- [18] E. Erdoğan, A. Küpçü, and A. E. Çiçek. Unsplit: Data-Oblivious Model Inversion, Model Stealing, and Label Inference Attacks against Split Learning. In *WPES*, page 115–124. ACM, 2022.
- [19] J. Fan and F. Vercauteren. Somewhat practical fully homomorphic encryption. *Cryptology ePrint Archive*, 2012.
- [20] D. Froelicher, J. R. Troncoso-Pastoriza, A. Pyrgelis, S. Sav, J. S. Sousa, J.-P. Bossuat, and J.-P. Hubaux. Scalable Privacy-Preserving Distributed Learning. *PoPETs*, (2):323–347, 2021.
- [21] J. Fu, X. Ma, B. B. Zhu, P. Hu, R. Zhao, Y. Jia, P. Xu, H. Jin, and D. Zhang. Focusing on Pinocchio's Nose: A Gradients Scrutinizer to Thwart Split-Learning Hijacking Attacks Using Intrinsic Attributes. *The Network and Distributed System Security Symposium*, 2023.
- [22] G. Gawron and P. Stubbings. Feature Space Hijacking Attacks against Differentially Private Split Learning. In *PPAI*, 2022.
- [23] R. Gilad-Bachrach, N. Dowlin, K. Laine, K. Lauter, M. Naehrig, and J. Wernsing. Cryptonets: Applying neural networks to encrypted data with high throughput and accuracy. In *ICML*, 2016.
- [24] O. Gupta and R. Raskar. Distributed learning of deep neural network over multiple agents. *Journal of Network and Computer Applications*, 116:1–8, 08 2018.
- [25] E. Hesamifard, H. Takabi, M. Ghasemi, and R. Wright. Privacy-preserving machine learning as a service. *PETS*, 2018.
- [26] B. Hitaj, G. Ateniese, and F. Perez-Cruz. Deep Models Under the GAN: Information Leakage from Collaborative Deep Learning. In *ACM CCS*, 2017.
- [27] B. Jayaraman, L. Wang, D. Evans, and Q. Gu. Distributed learning without distrust: Privacy-preserving empirical risk minimization. In *NIPS*, 2018.
- [28] P. Joshi, C. Thapa, S. Camtepe, M. Hasanuzzaman, T. Scully, and H. Afi. Performance and Information Leakage in Split Learning and Multi-Head Split Learning in Healthcare Data and Beyond. *Methods and Protocols*, 5(4):60, 2022.
- [29] T. Khan, K. Nguyen, and A. Michalas. A More Secure Split: Enhancing the Security of Privacy-Preserving Split Learning. In *Secure IT Systems*, pages 307–329. Springer, 2023.
- [30] T. Khan, K. Nguyen, and A. Michalas. Split Ways: Privacy-Preserving Training of Encrypted Data Using Split Learning. *arXiv preprint arXiv:2301.08778*, 2023.
- [31] T. Khan, K. Nguyen, A. Michalas, and A. Bakas. Love or Hate? Share or Split? Privacy-Preserving Training Using Split Learning and Homomorphic Encryption. In *PST*, pages 1–7. IEEE, 2023.
- [32] J. Konečný, H. B. McMahan, D. Ramage, and P. Richtárik. Federated Optimization: Distributed Machine Learning for On-Device Intelligence. *arXiv preprint arXiv:1610.02527*, 2016.
- [33] J. Konečný, H. B. McMahan, F. X. Yu, P. Richtárik, A. T. Suresh, and D. Bacon. Federated Learning: Strategies for Improving Communication Efficiency. *arXiv preprint arXiv:1610.05492*, 2017.
- [34] Y. Lecun, L. Bottou, Y. Bengio, and P. Haffner. Gradient-Based Learning Applied to Document Recognition. *Proceedings of the IEEE*, 86(11):2278–2324, 1998.
- [35] Y. LeCun and C. Cortes. MNIST handwritten digit database. 2010.
- [36] W. Li, F. Milletari, D. Xu, N. Rieke, J. Hancox, W. Zhu, M. Baust, Y. Cheng, S. Ourselin, M. J. Cardoso, and A. Feng. Privacy-preserving federated brain tumour segmentation. In *Springer MLMI*, 2019.

- [37] Z. Li, C. Yan, X. Zhang, G. Gharibi, Z. Yin, X. Jiang, and B. A. Malin. Split Learning for Distributed Collaborative Training of Deep Learning Models in Health Informatics. In *Annual Symposium Proceedings*, volume 2023, page 1047–1056. AMIA, 2023.
- [38] J. Liu, M. Juuti, Y. Lu, and N. Asokan. Oblivious neural network predictions via MiniONN transformations. In *ACM CCS*, 2017.
- [39] J. Liu, X. Lyu, Q. Cui, and X. Tao. Similarity-based Label Inference Attack against Training and Inference of Split Learning. *TIFS*, 2024.
- [40] Q. Lou, B. Feng, G. C. Fox, and L. Jiang. Glyph: Fast and Accurately Training Deep Neural Networks on Encrypted Data. In *NeurIPS*, volume 33, pages 9193–9202. Curran Associates, Inc., 2020.
- [41] V. Lyubashevsky, C. Peikert, and O. Regev. On ideal lattices and learning with errors over rings. In H. Gilbert, editor, *Advances in Cryptology – EUROCRYPT 2010*, pages 1–23, Berlin, Heidelberg, 2010. Springer Berlin Heidelberg.
- [42] U. Majeed, S. S. Hassan, and C. S. Hong. Vanilla Split Learning for Transportation Mode Detection using Diverse Smartphone Sensors. In *KCC*, pages 23–25. KIISE, 2021.
- [43] Y. Mao, Z. Xin, Z. Li, J. Hong, Q. Yang, and S. Zhong. Secure Split Learning Against Property Inference, Data Reconstruction, and Feature Space Hijacking Attacks. In *ESORICS*, pages 23–43. Springer, 2023.
- [44] W. S. McCulloch and W. Pitts. A logical calculus of the ideas immanent in nervous activity. *The bulletin of mathematical biophysics*, 5:115–133, 1943.
- [45] B. McMahan, E. Moore, D. Ramage, S. Hampson, and B. A. y Arcas. Communication-Efficient Learning of Deep Networks from Decentralized Data. In *Artificial Intelligence and Statistics*, volume 54. PMLR, 2017.
- [46] H. B. McMahan, D. Ramage, K. Talwar, and L. Zhang. Learning differentially private recurrent language models. *CoRR*, abs/1710.06963, 2018.
- [47] L. Melis, C. Song, E. De Cristofaro, and V. Shmatikov. Exploiting Unintended Feature Leakage in Collaborative Learning. In *SP*, pages 691–706. IEEE, 2019.
- [48] Message Passing Interface Forum. *MPI: A Message-Passing Interface Standard*. Message Passing Interface Forum, 1994. Version 1.0.
- [49] K. Nandakumar, N. Ratha, S. Pankanti, and S. Halevi. Towards Deep Neural Network Training on Encrypted Data. *CVPR*, 2019.
- [50] S. Navathe, S. Ceri, G. Wiederhold, and J. Dou. Vertical partitioning algorithms for database design. *ACM Transactions on Database Systems (TODS)*, 9(4):680–710, 1984.
- [51] S. B. Navathe and M. Ra. Vertical partitioning for database design: a graphical algorithm. In *Proceedings of the 1989 ACM SIGMOD international conference on Management of data*, pages 440–450, 1989.
- [52] U. Norman and A. E. Cicek. St-steiner: a spatio-temporal gene discovery algorithm. *Bioinformatics*, 35(18):3433–3440, 2019.
- [53] M. P. Parisot, B. Pejo, and D. Spagnuolo. Property Inference Attacks on Convolutional Neural Networks: Influence and Implications of Target Model’s Complexity. In *Proceedings of the 18th International Conference on Security and Cryptography - SECRYPT*, pages 715–721. INSTICC, SciTePress, 2021.
- [54] D. Pasquini, G. Ateniese, and M. Bernaschi. Unleashing the Tiger: Inference Attacks on Split Learning. In *SIGSAC CCS*, page 2113–2129. ACM, 2021.
- [55] A. Paszke, S. Gross, F. Massa, A. Lerer, J. Bradbury, G. Chanan, T. Killeen, Z. Lin, N. Gimelshein, L. Antiga, A. Desmaison, A. Kopf, E. Yang, Z. DeVito, M. Raison, A. Tejani, S. Chilamkurthy, B. Steiner, L. Fang, J. Bai, and S. Chintala. Pytorch: An imperative style, high-performance deep learning library. In *Advances in Neural Information Processing Systems 32*, pages 8024–8035, 2019.
- [56] G.-L. Pereteanu, A. Alansary, and J. Passerat-Palmbach. Split HE: Fast Secure Inference Combining Split Learning and Homomorphic Encryption. In *PPAI*, 2022.
- [57] L. T. Phong, Y. Aono, T. Hayashi, L. Wang, and S. Moriai. Privacy-preserving deep learning: Revisited and enhanced. In *Springer ATIS*, 2017.
- [58] L. T. Phong, Y. Aono, T. Hayashi, L. Wang, and S. Moriai. Privacy-preserving deep learning via additively homomorphic encryption. *IEEE TIFS*, 13(5):1333–1345, 2018.
- [59] M. G. Poirot. Split Learning in Health Care: Multi-center Deep Learning without sharing patient data. Master’s thesis, University of Twente, 2020.
- [60] M. G. Poirot, P. Vepakomma, K. Chang, J. Kalpathy-Cramer, R. Gupta, and R. Raskar. Split Learning for collaborative deep learning in healthcare. *arXiv preprint arXiv:1912.12115*, 2019.
- [61] W. H. Press, S. A. Teukolsky, W. T. Vetterling, and B. P. Flannery. *Numerical Recipes 3rd Edition: The Art of Scientific Computing*. Cambridge University Press, 2007.
- [62] M. Ra. Horizontal partitioning for distributed database design: A graph-based approach. In *Australian Database Conference*, pages 101–120, 1993.
- [63] M. A. Rahman, T. Rahman, R. Laganière, N. Mohammed, and Y. Wang. Membership inference attack against differentially private deep learning model. *Trans. Data Priv.*, 11(1):61–79, 2018.
- [64] D. Reich, A. Todoki, R. Dowsley, M. D. Cock, and A. C. A. Nascimento. Privacy-preserving classification of personal text messages with secure multi-party computation: An application to hate-speech detection. *CoRR*, abs/1906.02325, 2021.
- [65] D. E. Rumelhart, G. E. Hinton, and R. J. Williams. Learning representations by back-propagating errors. *nature*, 323(6088):533–536, 1986.
- [66] S. Satpathy, O. Khalaf, D. Kumar Shukla, M. Chowdhary, and S. Algburi. A collective review of Terahertz technology integrated with a newly proposed split learningbased algorithm for healthcare system. *International Journal of Computing and Digital Systems*, 15(1):1–9, 2024.
- [67] F. K. Satterstrom, J. A. Kosmicki, J. Wang, M. S. Breen, S. De Rubeis, J.-Y. An, M. Peng, R. Collins, J. Grove, L. Klei, et al. Large-scale exome sequencing study implicates both developmental and functional changes in the neurobiology of autism. *Cell*, 180(3):568–584, 2020.
- [68] S. Sav, A. Diaa, A. Pyrgelis, J.-P. Bossuat, and J.-P. Hubaux. Privacy-preserving federated recurrent neural networks. *PoPETs*, (4):500–521, 2021.
- [69] S. Sav, A. Pyrgelis, J. R. Troncoso-Pastoriza, D. Froelicher, J.-P. Bossuat, J. S. Sousa, and J.-P. Hubaux. Poseidon: Privacy-preserving federated neural network learning. In *Network and Distributed System Security Symposium (NDSS)*, 2021.
- [70] R. Shokri and V. Shmatikov. Privacy-preserving deep learning. In *ACM Conference on Computer and Communications Security (CCS)*, 2015.
- [71] R. Shokri, M. Stronati, C. Song, and V. Shmatikov. Membership inference attacks against machine learning models. In *2017 IEEE Symposium on Security and Privacy (SP)*, pages 3–18. IEEE, 2017.
- [72] Z. D. Stephens, S. Y. Lee, F. Faghri, R. H. Campbell, C. Zhai, M. J. Efron, R. Iyer, M. C. Schatz, S. Sinha, and G. E. Robinson. Big Data: Astronomical or Genomical? *PLoS Biology*, 13(7), 2015.
- [73] C. Thapa, P. C. M. Arachchige, S. Camtepe, and L. Sun. Splitfed: When federated learning meets split learning. In *Proceedings of the AAAI Conference on Artificial Intelligence*, volume 36, pages 8485–8493, 2022.
- [74] C. Thapa, M. A. P. Chamikara, and S. A. Camtepe. Advancements of Federated Learning Towards Privacy Preservation: From Federated Learning to Split Learning. *Federated Learning Systems: Towards Next-Generation AI*, pages 79–109, 2021.
- [75] T. Titcombe, A. J. Hall, P. Papadopoulos, and D. Romanini. Practical Defences Against Model Inversion Attacks for Split Neural Networks. In *ICLR Workshop on Distributed and Private Machine Learning (DPML)*, 2021.
- [76] S. Truex, N. Baracaldo, A. Anwar, T. Steinke, H. Ludwig, R. Zhang, and Y. Zhou. A hybrid approach to privacy-preserving federated learning. In *ACM AISec*, 2019.
- [77] P. Vepakomma, O. Gupta, T. Swedish, and R. Raskar. Split learning for health: Distributed deep learning without sharing raw patient data. In *ICLR AI for social good workshop*, 2019.
- [78] S. Wagh, D. Gupta, and N. Chandran. SecureNN: 3-Party Secure Computation for Neural Network Training. *PETS*, 2019.
- [79] S. Wagh, S. Tople, F. Benhamouda, E. Kushilevitz, P. Mittal, and T. Rabin. FALCON: Honest-majority maliciously secure framework for private deep learning. *PETS*, 2020.
- [80] P. Wagner, N. Strodthoff, E. Bietti, T. Schaeffter, X. Zhu, and R. Durichen. Ptb-xl, a large publicly available electrocardiography dataset. *Scientific Data*, 2020.
- [81] W. Wang, T. Wang, L. Wang, N. Luo, P. Zhou, D. Song, and R. Jia. DPliis: Boosting Utility of Differentially Private Deep Learning via Randomized Smoothing. *PETS*, 2021.
- [82] K. Wei, J. Li, M. Ding, C. Ma, H. H. Yang, F. Farokhi, S. Jin, T. Q. S. Quek, and H. V. Poor. Federated learning with differential privacy: Algorithms and performance analysis. *IEEE Transactions on Information Forensics and Security*, 15:3454–3469, 2020.
- [83] N. Wu, F. Farokhi, D. Smith, and M. A. Kaafar. The value of collaboration in convex machine learning with differential privacy. *CoRR*, abs/1906.09679, 2019.
- [84] Y.-c. Wu and J.-w. Feng. Development and Application of Artificial Neural Network. *Wireless Personal Communications*, 102:1645–1656, 2018.
- [85] X. Yang, J. Sun, Y. Yao, J. Xie, and C. Wang. Differentially private label protection in split learning. *arXiv preprint arXiv:2203.02073*, 2022.
- [86] I.-C. Yeh and C. hui Lien. The comparisons of data mining techniques for the predictive accuracy of probability of default of credit card clients. *Expert Systems with Applications*, 36(2):2473 – 2480, 2009.

- [87] F. Yu, L. Wang, B. Zeng, K. Zhao, Z. Pang, and T. Wu. How to backdoor split learning. *Neural Networks*, 168:326–336, 2023.
- [88] F. Yu, L. Wang, B. Zeng, K. Zhao, T. Wu, and Z. Pang. SIA: A sustainable inference attack framework in split learning. *Neural Networks*, 171:396–409, 2024.
- [89] F. Yu, B. Zeng, K. Zhao, Z. Pang, and L. Wang. Chronic Poisoning: Backdoor Attack against Split Learning. In *Proceedings of the AAAI Conference on Artificial Intelligence*, volume 38, pages 16531–16538, 2024.
- [90] C. Zhang, S. Li, J. Xia, W. Wang, F. Yan, and Y. Liu. Batchcrypt: Efficient homomorphic encryption for cross-silo federated learning. In *Proceedings of the 2020 USENIX Conference on Usenix Annual Technical Conference*, USENIX ATC’20, USA, 2020. USENIX Association.
- [91] Q. Zhang, Z. Jiang, Q. Lu, J. Han, Z. Zeng, S.-H. Gao, and A. Men. Split to Be Slim: An Overlooked Redundancy in Vanilla Convolution. In *IJCAI*, 2020.
- [92] W. Zheng, R. A. Popa, J. E. Gonzalez, and I. Stoica. Helen: Maliciously secure cooperative learning for linear models. In *IEEE S&P*, 2019.
- [93] H. Zhu, R. S. Mong Goh, and W.-K. Ng. Privacy-preserving weighted federated learning within the secret sharing framework. *IEEE Access*, 8:198275–198284, 2020.
- [94] L. Zhu, Z. Liu, and S. Han. Deep leakage from gradients. In *Proceedings of the 33rd International Conference on Neural Information Processing Systems*, pages 14774–14784, 2019.